Applying Sensor Uncertainty Mitigation Schemes to Detect-and-Avoid Systems

Michael Abramson* and Mohamad Refai †
Crown Consulting, Inc., Moffett Field, California, 94035

M. Gilbert Wu ‡ and Seungman Lee§
NASA Ames Research Center, Moffett Field, California, 94035

Impact of sensor noise on the performance of Detect-And-Avoid (DAA) systems can be reduced by implementing various mitigation schemes. This paper evaluates the Sensor Uncertainty Mitigation (SUM) method, implemented in the Detect and Avoid Alerting Logic for Unmanned Systems (DAIDALUS) algorithm, a reference implementation in the DAA minimum operational performance standards. DAIDALUS SUM performance is evaluated using a few safety and operational suitability metrics and compared with more traditional approaches using static safety buffers. A large number of encounters representative of low-speed unmanned aircraft against non-cooperative manned aircraft are simulated and evaluated. An air-to-air radar model produces representative sensor noise for the DAA system. Results show that increasing the tunable parameters for horizontal and vertical uncertainty in DAIDALUS SUM improves the safety metric at the cost of increasing the number of system alerts leading to increased workload. A range of SUM parameters is recommended as suitable values for the type of operations considered for this work. General trends and optimal SUM configurations were found to be nearly the same for two large and very different encounter data sets.

Nomenclature

ADS-B	Automatic Dependent Surveillance – Broadcast
AST	active surveillance transponder
ATAR	air-to-air radar
CPA	closest point of approach
CPDS	Conflict Prediction and Display System
DAA	detect-and-avoid
DAIDALUS	Detect and Avoid Alerting Logic for Unmanned Systems
DWC	DAA Well Clear
FOV	field of view
GPS	Global Positioning System
GRACE	Generic Resolution Advisor and Conflict Evaluator
h*	vertical separation threshold
HITL	human-in-the-Loop
HMD*	horizontal miss distance threshold
JADEM	Java Architecture for DAA Extensibility and Modeling
LoDWC	loss of DAA well clear
MATG	Multimodal Adaptable Trajectory Generator
MOPS	Minimum Operational Performance Standards

*Senior Engineer, M/S 210-8, AIAA Member, michael.abramson@nasa.gov
†Senior Engineer, M/S 210-8, mohamad.s.refai@nasa.gov
‡Aerospace Engineer, Aviation Systems Division, M/S 210-10, AIAA Member, gilbert.wu@nasa.gov
§Aerospace Engineer, Aviation Systems Division, M/S 210-8, Senior AIAA Member, seungman.lee@nasa.gov

NAS	National Airspace System
SLoWC	severity of loss of Well Clear
SUM	Sensor Uncertainty Mitigation
SWaP	size, weight, and power
UA	unmanned aircraft
UAS	unmanned aircraft systems
VFR	visual flight rules
VISA	Virtual Intruder State Aggregation
WCR	Well Clear Recovery
N_{pa}	number of pilot action count per encounter
S	weighted average performance index over all metrics
s_k	performance index for k^{th} metric
$t_{\text{WCR-LoDWC}}$	average time between unmitigated WCR and LoDWC

I. Introduction

SUCCESSFUL integration of Unmanned Aircraft Systems (UAS) into the National Airspace System (NAS) is predicated upon maintaining or exceeding the level of safety and performance achieved by current operations [1]. RTCA Special Committee 228 (SC-228) is developing UAS Minimum Operational Performance Standards (MOPS) to achieve this goal. These MOPS define the Detect-And-Avoid function [2], which comprises three sub-functions, namely, detection, alerting, and guidance. In addition the MOPS introduce an algebraic definition of what it means to be Well Clear of other aircraft, referenced hereinafter as DAA Well Clear (DWC).

The DAA Detect function uses onboard or ground surveillance systems to detect traffic. Of particular relevance is the ability to detect non-cooperative traffic, such as aircraft flying visual flight rules (VFR) that do not have a broadcasting transponder or ADS-B system. The MOPS require an onboard air-to-air radar (ATAR) for this purpose (see [3] for ATAR requirements). The Alerting and Guidance functions provide notification of potential hazards that may arise with detected aircraft, and the solutions available to avoid or mitigate observed hazards.

One of the key challenges in implementing effective DAA systems, is sensor noise. The effects of sensor noise are varied and may include loss of alerting and guidance stability. Alerting, for example, may flicker while guidance may exhibit distracting fluctuations. For a pilot-in-control concept of operation, which is adopted in the MOPS, this can be detrimental to effective mitigation of hazards. Furthermore, different sensor systems may exhibit distinctly different noise characteristics. For example, a mode-C transponder does not measure bearing of another aircraft (an intruder) relative to the UA controlled by the UAS pilot (ownship), whereas an ATAR does. DAA systems must take sensor noise characteristics into account.

Several schemes for mitigating the effects of noise are possible. A tracker may be used, for example, to provide correlated smoothed intruder states [4–11], which are then used to predict hazards. Another approach would generate multiple belief states assigning each state a likelihood using known noise characteristics and using a decision process to predict hazards [12, 13]. Yet another approach might use a buffer to inflate desired separation thresholds, thus providing more conservative hazard predictions [14]. One may also impose alerting persistence requirements or may delay the onset of an alert until a certain number of hazards are reported in a given period of time for each intruder [2]. These methods and others are not mutually exclusive and may be used in combination to achieve desired DAA performance.

This paper investigates the benefits of using sensor uncertainty information in a Sensor Uncertainty Mitigation (SUM) method, which is implemented in the Detect and Avoid Alerting Logic for Unmanned Systems (DAIDALUS), the reference algorithm adopted in the MOPS. DAIDALUS SUM performance is compared with separation buffers using the same safety and operational suitability metrics. Closed loop DAA simulations incorporating UAS pilot resolutions are used, with SUM parameters being the independent variables. Open loop alerting-only simulations are also used to assess open-loop alerting metrics.

The paper is organized as follows. The next section provides a high-level background on DAA systems. Section III provides overview of previous work related to sensor uncertainty mitigation methods. Section IV describes the approach used to evaluate SUM performance. Section V describes the main results. Finally, concluding remarks are presented in Section VI.

II. Background on Detect-and-Avoid

The DAA system assists UAS operators and pilots in maintaining separation with other aircraft. One of the core challenges of such capability is to meet FAA requirements to "see and avoid" and when passing other aircraft to remain "well clear" as mandated for manned aircraft in 14 CFR §91.113 [15]. UAS pilots are not in the flight deck to "see and avoid," so pilots must rely on surveillance and algorithms for conflict detection and avoidance. In this situation, the separation standard, or the DWC, must have a quantitative definition. To provide information for maintaining DWC, the DAA system computes alerts and guidance based on a look-ahead time of 1 to 2 minutes. The alerting and guidance structure is designed with the assumptions that a UAS flies by instrument flight rules (IFR) and UAS operators or pilots are "in the loop" for decision making.

The study applies a DWC that is to be defined in an upcoming revision of the DAA MOPS for en-route encounters with non-cooperative intruders, i.e., VFR aircraft without a broadcasting transponder or ADS-B out system. Encounters with non-cooperative intruders pose unique challenges because of sensor noise and especially large vertical state uncertainty typical for ATAR. This study focuses on the DAA system's performance against non-cooperative intruders in an operational environment representative of UAS with low size, weight, and power (SWaP) sensors, i.e., low speed unmanned aircraft (UA) and a limited surveillance range (see Section IV for more details). The DWC for a non-cooperative intruder is a short cylinder (a "hockey puck") with a horizontal radius of 2,200 ft and a vertical threshold of 450 ft above and below the UA [16].

The DAA MOPS define three types of alerts in increasing levels of severity: preventive, corrective, and warning. The medium level, corrective, alert indicates that a loss of DAA well clear (LoDWC) is predicted to occur in the future, an avoidance maneuver is necessary, but there is still time for coordination with air traffic control (ATC). The highest level, warning, alert indicates that a LoDWC is imminent, an avoidance maneuver is needed, and coordination with ATC before maneuvering is not a requirement. The lowest level, preventive alert, effectively has the same thresholds and alerting times as a corrective alert, but with larger vertical separation between 450 to 700 feet. This alert should not be triggered by non-cooperative aircraft (due to the lack of precise altitude information) and is not modeled in this study.

The DAA system must present maneuver guidance to UAS pilots in the form of DWC-based, conflict-free aircraft headings or altitude ranges, or "bands." In case a LoDWC is imminent, these bands become "saturated," meaning there are no conflict free headings or altitudes and that a loss of DWC is unavoidable no matter what action a UAS pilot takes. In this case the DAA system should present Well Clear Recovery (WCR) guidance. This is a range of headings or altitudes that, if executed, can increase separation at CPA and regain DWC effectively. Figure 1 depicts a mockup of guidance to remain and regain DWC. In this figure red (warning) or yellow (corrective) represent the ranges of headings or altitudes that will result in a LoDWC, and green depicts the guidance that will (a) avoid a LoDWC or (b) effectively regain DWC.

(a) Guidance to Remain Well Clear

(b) Guidance to Regain Well Clear
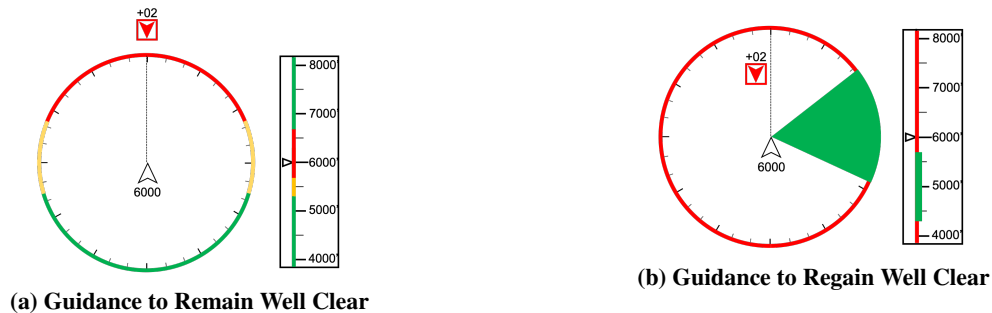
Fig. 1 Guidance Display Examples

Several alerting and guidance algorithms have been developed to support research, development, and evaluation of DAA MOPS. One of the first such algorithms was implemented in General Atomics' Conflict Prediction and Display System (CPDS) that included a UAS pilot display with conflict probing [17]. CPDS was extensively used in flight tests with the Ikhana vehicle, a variant of MQ-9.

NASA developed the Generic Resolution Advisor and Conflict Evaluator (GRACE) alerting and guidance algorithm, which combined flexibility, robustness, and computational efficiency [18]. GRACE was used in a number of real-time and fast-time experiments, including parametric studies, NAS-wide simulations, human-in-the-loop experiments, and live flight tests. Another alerting and guidance algorithm, Detect and Avoid Alerting Logic for Unmanned Systems

(DAIDALUS)[19], was developed by NASA specifically to support Phase 1 MOPS [2]. DAIDALUS uses closed-form solutions to compute alerting and guidance.

The recently developed Aircraft Collision Avoidance System X (ACAS-X) [12] is envisioned by the Federal Aviation Administration (FAA) as a replacement for the currently deployed Traffic Alert and Collision Avoidance System II (TCAS-II) [20]. The UAS-variant of ACAS-X, called ACAS-Xu, is being developed to meet the requirements defined by the SC-228 in DO-365 [2].

III. Sensor Uncertainty Mitigation Methods

A. Mitigation Schemes

The first "line of defense" against sensor noise is improving stability of aircraft states used in DAA algorithms. The MOPS define a fusion tracker that can correlate and fuse measurements from multiple sensors such as ADS-B, active surveillance, and ATAR. This tracker can potentially implement various filtering algorithms such as multi-state filtering [4–8], alpha-beta filter [9], different versions of Kalman filter [10], and other filters [4, 11]

For conflict avoidance systems, a common approach to mitigating sensor noise and other sources of uncertainty in aircraft states involves adding spatial or temporal safety buffers. An example of such an approach for UAS DAA systems can be found in [14]. This method is simple and effective, but it has its limitations. For example, large safety buffers may increase the likelihood of incorrect alerts defined in DAA MOPS as alerts issued when the intruder aircraft remains in the Non-Hazard Zone, where DAA must not alert [2]. This can lead to unnecessary maneuvers, therefore increasing workload.

The DAA MOPS include an alert hysteresis requirement, which aims to reduce undesired alert flickering [2]. The requirement is that an alert "shall persist for a minimum of four seconds, unless the intruder is declared a higher priority alert." In addition, the MOPS also suggest the use of an M of N ($M < N$) alert filter, which requires that an alert must be present in at least M of N consecutive detection cycles, in order for the alert to be valid. The effect is to delay alerting and guidance displayed to the UAS pilot until the alerts have sufficiently stabilized.

The use of hysteresis or M of N, however, cannot mitigate gradual changes in alerts caused by low-frequency components of tracker noise, or by maneuvering aircraft, or both. Furthermore, they do not address the issue of guidance fluctuations, which may confuse a UAS pilot or lead to erroneous maneuvers. One approach to addressing this issue would be to apply persistence logic for guidance in the same way as it was used for alerts.

A more reliable way to suppress the abrupt guidance changes is by using a cost/reward function that allows a flexible balance between guidance stability and other considerations. This idea was implemented in two different algorithms that demonstrated robust performance under simulated sensor uncertainties [18, 21]: GRACE [18] and ACAS and its derivatives [13].

If sensor uncertainty information is available in real time, it can be used to improve alerting and guidance stability. For instance, ACAS-Xu utilizes this information in computation of its belief states. The Sensor Uncertainty Mitigation (SUM) capability, recently added to DAIDALUS, also follows a similar approach. DAIDALUS SUM, which will be described in Subsection III.B, is the focus of this study.

B. DAIDALUS SUM

DAIDALUS SUM uses sensor uncertainty information to compute bounds on the errors in the aircraft position and velocity vectors [22]. These bounds are used to create "phantom" intruders, which are then used to compute alerting and guidance by combining the results for each phantom with those for the sensed intruder. This approach is effectively creating a "dynamic" buffer, which is reevaluated with every detection cycle.

SUM requires six tunable parameters. Three of these parameters are z-scores indicating the number of standard deviations to consider for horizontal and vertical position uncertainty and for vertical velocity uncertainty:

h_pos_z   number of standard deviations for horizontal position uncertainty

v_pos_z   number of standard deviations for vertical position uncertainty

v_vel_z   number of standard deviations for vertical velocity uncertainty

The other three tunable parameters for horizontal velocity uncertainty are:

h_vel_z_score_min	number of standard deviations for horizontal velocity uncertainty at high distance
h_vel_z_score_max	number of standard deviations for horizontal velocity uncertainty at low distance
h_vel_z_distance	distance at which to start phasing between the high distance and low distance values

The use of the last three parameters requires some clarification. SUM allows using a smaller velocity uncertainty when the aircraft are further apart because a slight change in the size of the velocity error at those distances can produce a very large set of possible future states as those velocities are propagated in time. This problem is mitigated by allowing the horizontal velocity uncertainty, expressed as a number of standard deviations, to decrease as the aircraft get further apart.

For given level of sensor noise, larger z-scores have the effect of increased "dynamic buffers" around a "sensed" intruder. Larger z-scores are therefore expected to make alerts and bands more stable. At the same time, alerts may be issued earlier, and the probability of incorrect alerts may increase. Furthermore, using large z-scores may result in wider bands that may become saturated earlier than necessary. Increasing z-scores will therefore result in increasingly conservative guidance, which may cause pilots to use more aggressive or excessive maneuvers.

Evaluation of an earlier version of SUM using a limited number of encounters was conducted in [23–25]. The main alerting metric used for evaluation was Alert Jitter, which is defined as the average number of transitions to alerts of higher severity (e.g. from corrective to warning alerts) that occur within an encounter set. The effectiveness of guidance was evaluated using Severity of Loss of Well Clear (SLoWC) metric, capturing the most serious instance of LoDWC throughout an encounter. SLoWC ranges from 0% (DAA Well Clear maintained throughout the encounter) to 100% (mid-air collision). Results showed improvement in alert stability and safety metrics with SUM. However, the tunable SUM parameters in all these studies varied only within narrow ranges. Also, the small number of encounters simulated (< 300) was not enough for accurate estimates of safety metrics such as the SLoWC. Moreover, the optimal values of these parameters may be very different if more metrics are used and if Phase 2 requirements for aircraft and sensor performance are assumed, such as lower aircraft speeds, faster turn rates, and shorter radar range. The need to find most suitable values of these parameters for Phase 2 DAA MOPS motivated this study.

IV. Approach

A. Simulation Architecture

The simulations in this study are conducted using the Java Architecture for DAA Extensibility and Modeling (JADEM), developed by NASA to support evaluation of different DAA concepts and their safety characteristics [18]. Figure 2 depicts the simulation architecture used. The components in the figure are described in more detail in subsections IV.D–IV.G below.
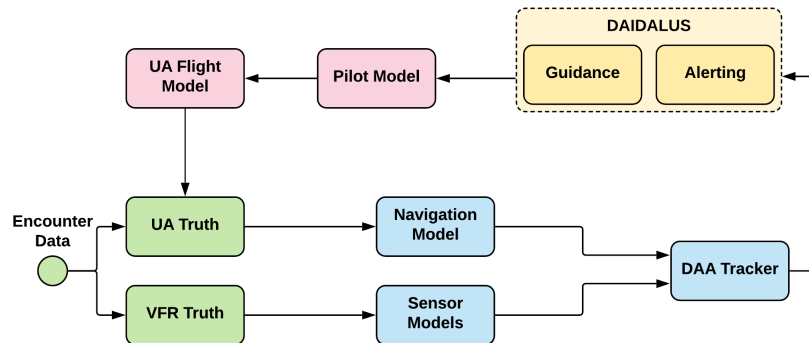
Fig. 2   Simulation Architecture

B. Metrics

Three metrics are analyzed in this study:
1) Severity of Loss of Well Clear (SLoWC) ratio, defined as the ratio of weighted averages of SLoWC between

mitigated and unmitigated runs for the same encounter set and configuration. The advantage of this metric is that it captures not only the number of LoDWC events, but also how "severe" (i.e. close to NMAC) these events were. The lower value of SLoWC ratio indicates that the UAS pilot is more successful in avoiding the LoDWC, and if the losses of DWC cannot be avoided, the pilot maneuvers make them less dangerous.

2) Number of UAS pilot actions (i.e. evaluation, selection, and execution of maneuvers) per encounter, denoted as N_{pa}. This metric can be used to characterize the workload. It also may have implications for safety due to the factors that are not captured by DAA pilot model used in this study. For instance, it's conceivable that excessive maneuvering caused by more conservative guidance may increase UAS pilot fatigue and probability of wrong decisions.

3) Average time between the well clear recovery (WCR) time and the time of LoDWC, denoted as $t_{\text{WCR-LoDWC}}$. For operational reasons, $t_{\text{WCR-LoDWC}}$ shouldn't be too large because WCR presents a risky situation in which pilots are given limited guidance, which should not be displayed earlier than necessary. Since the maneuver time needed to resolve a conflict is typically from 10 to 20 seconds [2], it is assumed that WCR to LoDWC time should not exceed 20 seconds.

C. Encounters

The study used more than 80,000 pairwise encounters generated from projected UAS mission profiles developed under prior work [26], but modified for low SWaP UAS, and recorded radar traffic data that include visual flight rules and non-cooperative flights [27]. The encounters have the following properties when the aircraft are at their closest point of approach (CPA):

- ownship's true airspeed is below 110 KTAS.
- intruder's true airspeed is below 170 KTAS, a 95 percentile upper bound for non-cooperative aircraft [28].
- ownship's altitude is below 11000 feet.

More details about the encounters can be found in [29].

D. Sensor and Tracker Models

For this study, the intruders' simulated trajectory states, referred hereafter as "truth" states, were perturbed by a radar model with a vertically cylindrical radar field of view (FOV) with a radius of 3 NM, representative of the range of a low SWaP radar. Analysis with this type of FOV sheds light on the sensitivity of the DAA performance metrics to a finite surveillance range, a critical question for UAS operations with low SWaP sensors. Representative values used for azimuth and elevation errors were $0.5° \pm 1.0°$ and those for (slant) range error were 15 ± 21 meters. The Phase 1 MOPS require a tracker that fuses and correlates measurements from multiple sensors for a single intruder into tracks. The UA's state is also input into the tracker to produce the intruder's state in absolute coordinates. A fusion tracker developed by Honeywell [30] is used for this work. This tracker outputs the intruder's track position and velocity as well as estimated accuracies of the track.

E. Alerting and Guidance Algorithm

For this study, DAIDALUS is configured to issue a corrective alert 60 seconds and a warning alert 30 seconds before the UA is predicted to enter the conflict zone. Upon alerting, DAIDALUS generates corresponding preventive, corrective, and warning guidance indicating a range of conflict-free headings and altitudes for UAS pilot to select from in order to maintain DWC separation. In the absence of alerts, DAIDALUS computes peripheral guidance by projecting candidate vertical and horizontal DAA maneuvers into future times to determine which would result in conflicts. DAIDALUS also computes regain DWC guidance, or well clear recovery (WCR), if a LoDWC is unavoidable.

The alert conflict zone is based on the DWC and adds a buffer around it. For runs with a static buffer, the DWC's horizontal radius, or the horizontal miss distance threshold (HMD*) is scaled by a factor of 1.52 to be consistent with the parameters referenced in the Phase 1 MOPS. The vertical threshold, h*, is 450 ft in one configuration and 4000 ft in another. The 450 ft value is equal to the vertical threshold of the DWC as defined in the MOPS. The 4000 ft value is a conservative threshold suggested by the Phase 1 MOPS to guard against the large vertical state noise of an ATAR detecting non-cooperative aircraft. All runs with DAIDALUS SUM use the unbuffered HMD* = 2200 ft and vertical threshold h* = 450 ft.

F. Pilot Response Model

The DAA MOPS reference pilot response model calibrated from UAS pilot performance data obtained in the Human-in-the-Loop (HITL) simulations [29] was used to select maneuvers from DAA guidance and execute them. Appropriate delays at various states are applied to mimic the air traffic coordination time and pilot evaluation time. More details are described in [29]. Only horizontal maneuvers are used because large vertical state errors make vertical maneuvers less robust.

G. UA Flight Model

Once the UAS pilot response model selects a DAA maneuver and the execution delay elapses, the flight model takes control and modifies the UA's truth trajectory in accordance with the DAA maneuver. JADEM's flight model is based on Multimodal Adaptable Trajectory Generator (MATG) [18], a fast and flexible kinematic trajectory predictor. MATG can handle any constraints (position, heading, speed, altitude, vertical speed, and time) in any combination. The UA kinematics can be modeled using either bank angle or turn rate and vertical speeds that can be defined as functions of altitude and flight phase (climb/descent). When MATG is used for modeling pilot maneuvers, the target heading or altitude constraint is created from the output of DAA pilot model. Once the flight model has achieved the target heading or altitude, the UA trajectory retains it until the end of the encounter. The intruder's trajectory remains unchanged.

In this study, the DAA pilot model provided only heading guidance, and constant turn rate 7 deg/sec was assumed for all UA maneuvers.

H. Experiment Setup

Evaluating the effectiveness of sensor uncertainty mitigation necessitates comparisons between the following scenario configurations:

1) *Perfect*: the baseline case with "perfect" surveillance data without simulated sensor errors but with limited FoV representative of low SWaP airborne radar.
2) *Noisy*: similar to the perfect case but uses sensor and tracker model developed by Honeywell [30], for airborne radar with the same FoV.
3) *Mitigated*: similar to the noisy case but configured to use one or more noise mitigation methods, such as static buffers, or DAIDALUS SUM with different tunable parameters.

Perfect, noisy, and each of the mitigated configurations required two runs: "open loop," was used to generate metrics without applying a UAS pilot response model (see Section IV.F for more details), and "closed loop" with the application of the UAS pilot response model.

This section presents results for the following *Mitigated* configurations, compared with *Perfect* and *Noisy* configurations as defined in IV.H:

1) **HMD* buffer**: the HMD threshold was set to 3342 ft, replacing the standard 2200 ft HMD threshold.
2) **HMD* & Vert. buffer**: in addition to the HMD* buffer, the vertical threshold was set to 4000 ft, to protect against large radar errors in vertical state.
3) **SUM**: DAIDALUS SUM with different combinations of horizontal and vertical tunable parameters.

For **SUM** configurations, the following assumptions were made for SUM parameters:

- h_vel_z_score_max = h_pos_z_score
- h_vel_z_distance = 3.0 nmi
- h_vel_z_score_max / h_vel_z_score_min = 5
- v_vel_z_score = v_pos_z_score

This leaves only two independently varying parameters to generate a 2D map of performance metrics for **SUM** configurations: horizontal and vertical position z_scores.

I. Performance Evaluation

This study attempts to compare the overall performance of each simulation configuration via a single cost function by combining the aforementioned three metrics defined in Subsection IV.B. This approach is generally challenging and subjective. Nonetheless, this attempt will demonstrate the trade space between metrics and determine a reasonable range of SUM parameters.

To facilitate the construction of this cost function, the performance indices s_k were calculated for all metrics. The lower values of these indices always indicate the better performance. For the first two metrics, SLoWC ratio and

N_{pa}, s_k was defined simply as the ratio of value m_k of kth metric for given configuration to its value $m_{k,noisy}$ for *Noisy* configuration:

$$s_k = \frac{m_k}{m_{k,noisy}}, k = 1, 2 \tag{1}$$

The *Noisy* configuration is used as the denominator because this is the case without mitigation that can be used as a natural reference.

The last metric, $t_{\text{WCR-LoDWC}}$, couldn't be normalized the same way since it represented a penalty applied only for a time exceeding 20 second limit. Hence, its s_k was calculated as:

$$s_k = \frac{max(m_k - m_{k,limit}, 0)}{0.1 * m_{k,limit}}, k = 3 \tag{2}$$

This ensured that s_k was zero when the m_k is below 20 second limit $m_{k,limit}$, and it rapidly increased once the m_k exceeded $m_{k,limit}$.

The overall performance index S for each configuration was calculated simply by averaging s_k for all metrics with weights w_k reflecting the relative importance of each metric.

$$S = \sum_k w_k s_k \tag{3}$$

This allowed to compare overall performance across configurations. Section V provides a summary of evaluation results.

V. Results

The results for statistical metrics for buffered and SUM configurations in this section are shown as bar charts with error bars.

Figure 3 shows the LoWC Severity ratio for different mitigation methods compared to the unmitigated noisy configuration. Even for perfect configuration, the LoWC severity ratio is not zero because even with accurate information about intruder states, the losses of DWC could not always be avoided when intruders maneuvered unexpectedly. The LoWC Severity ratio for unmitigated noisy configuration is at the level of 16%, more than two times higher than for perfect configuration. This level of LoWC Severity ratio for worst case of noisy surveillance without any mitigation is too high and not operationally acceptable. All mitigation methods substantially reduce the LoWC Severity ratio compared to the unmitigated noisy configuration. The HMD* buffer reduces the LoWC Severity ratio two times, from 16.2% to 8.01%, and the combined HMD* and vertical buffer reduces it even further to 6.5%, comparable with best results for SUM. SUM results show a clear trend of reducing LoWC Severity ratio for increasing horizontal and vertical z_scores. The lowest SLoWC ratios are achieved at horizontal position z_score above 3 and vertical position z_scores 1 or higher, when SUM alerting and guidance become more conservative. Further increase in vertical z_score has little impact because the additional encounters affected by the increasing "dynamic" vertical buffer in SUM have little chance to become the LoDWC.

The reduction in SLoWC ratios is achieved at the cost of earlier alerts and higher likelihood of incorrect alerts. This results in higher values of N_{pa} as shown in Figure 4. All mitigation methods increase N_{pa}, and the most conservative SUM alerting and guidance increases it more than two times compared to noise without mitigation. In other words, pilots may have to work harder to achieve a slightly lower LoWC severity. This increase in workload is expected as was discussed in Subsection IV.B. Note that the vertical buffer and the increase in vertical z_score above 2 have only modest effect because the additional encounters affected by larger static or "dynamic" (in SUM) vertical buffer have a smaller chance to become the LoDWC.

Figure 5 shows that $t_{\text{WCR-LoDWC}}$ increases more than two-fold when horizontal static buffer is used, and nearly triples when SUM horizontal z_score increases from 1 to 5. This is a result of early saturation of heading bands for larger horizontal buffers, whether they are static or "dynamic" in SUM. Note that sensor noise by itself has very little effect on band saturation, hence the values of $t_{\text{WCR-LoDWC}}$ for perfect and noisy configurations are similar. More importantly, $t_{\text{WCR-LoDWC}}$ remains below acceptable 20 second limit only for SUM with horizontal position z_score below 3. This indicates that, irrespective of trade-off between SLoWC ratio and N_{pa}, using SUM with horizontal z_score higher than 3 will be problematic, since it will allow WCR guidance to appear too early.

Since all three metrics tell different stories, it is tempting to pursue an overall, or "combined," performance index for each configuration using Equation (3) with particular metric weights. Any choice of these weights is inherently

8
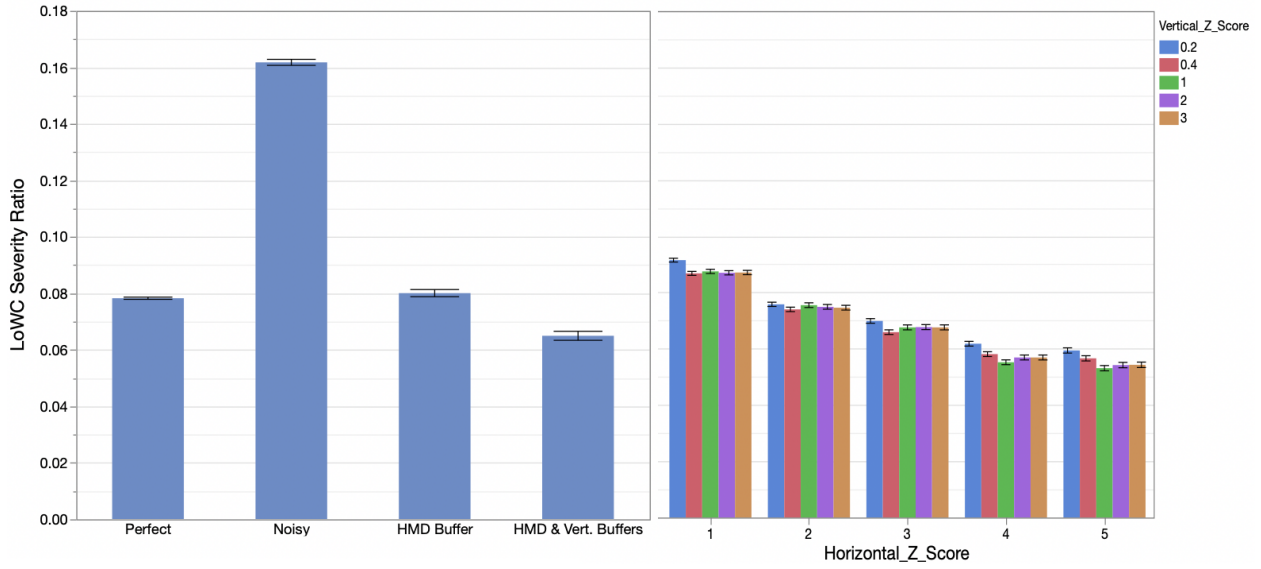
Fig. 3   Metrics for LoWC Severity Ratio
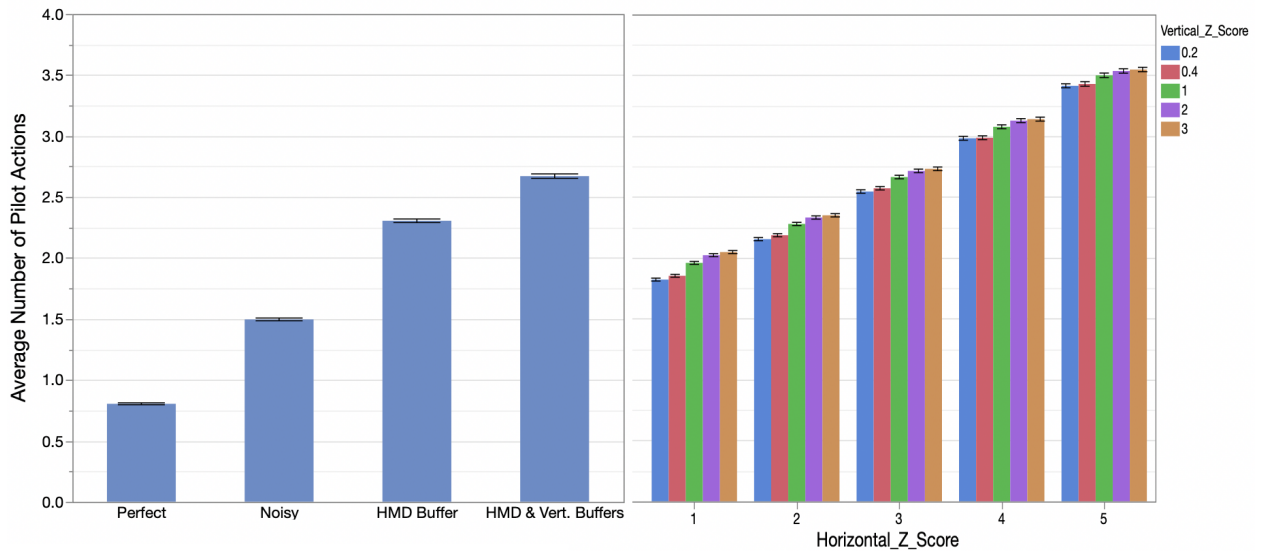
Fig. 4   Metrics for N_{pa}

subjective, but for the data in this study it was found that performance profile for different configurations and the optimal DAIDALUS SUM parameters were insensitive to weights within a wide range of "reasonable" metric weights. Figure 6 illustrates one such choice. Since safety outweighs any operational suitability considerations, the weight of SLoWC ratio w_1 is set to 1 while the weights of N_{pa} and $t_{\text{WCR-LoDWC}}$ are ten times lower: $w_2 = w_3 = 0.1$. With this choice, the combined performance index S for each configuration is shown in Figure 6 as a color map with blue and red colors representing the lower (preferred) and the higher values respectively. From this Figure it becomes clear that the best mitigation method is SUM with the horizontal position z_score equal 2 and vertical position z_score 0.4. Nonetheless, the overall combined performance index is fairly insensitive to the vertical z_score. Configurations with static buffers have slightly higher values of S than the optimal SUM configuration, but they perform better than SUM configurations
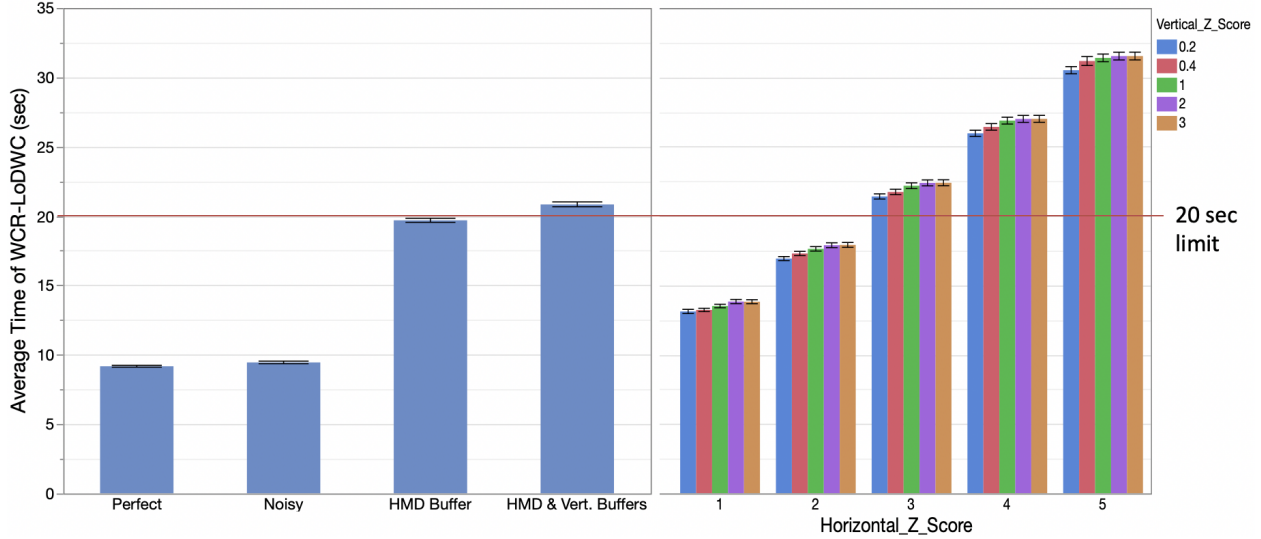
Fig. 5 Metrics for $t_{\text{WCR-LoDWC}}$

	buffers		SUM				
	HMD	HMD & vert.	horizontal pos z_score				
	0.54	0.52	1	2	3	4	5
0.2			0.57	0.51	0.56	0.73	0.93
0.4			0.55	0.50	0.56	0.73	0.95
1			0.56	0.52	0.59	0.74	0.94
2			0.56	0.52	0.60	0.76	0.96
3			0.56	0.51	0.60	0.76	0.96

vertical pos z_score

Fig. 6   Weighted Average Performance Indices S over All Metrics

with the horizontal z_score other than 2. This may indicate that static buffers used in this study provide a reasonably good approximation for average sensor noise. For different surveillance the advantage of SUM over static buffers may become more pronounced. Since values of all three metrics are subject to a certain level of error due to the finite number of encounters sampled, all SUM configurations with a horizontal position z_score equal to 2 as well as the HMD* plus vertical buffer configuration are all considered performing reasonably well.

Another set of simulations was performed for nearly 200,000 uncorrelated encounters provided by MIT Lincoln Laboratory [31]. General trends and optimal SUM configuration for this larger and very different encounter data set were found to be nearly the same as for NAS-wide encounters that were presented in this section.

VI. Summary and Concluding Remarks

Sensor uncertainties may impact the performance of Detect-and-Avoid (DAA) systems. This paper evaluated the effectiveness of two static buffers and Sensor Uncertainty Mitigation (SUM) scheme implemented in the Detect and Avoid Alerting Logic for Unmanned Systems (DAIDALUS). Analysis focused on encounters involving unmanned aircraft with speeds below 110 KTAS flying below 11000 feet and non-cooperative aircraft with speeds below 170 KTAS detected by an airborne radar. Both open and closed-loop simulations, the latter involving a UAS pilot response model, were performed on more than 80,000 encounters.

Three metrics were defined and computed for evaluating the effectiveness of horizontal and vertical buffers and DAIDALUS SUM in mitigating the impact of sensor noise. Results show a trade space between safety and operational

suitability metrics. It was determined that DAIDALUS SUM performance was the best for a horizontal z_score equal to 2, or two standard deviations for horizontal position and velocity uncertainty, and it was relatively insensitive to vertical z_score parameters. The static buffers runs also achieve comparable performance. These results were found to be robust with respect to the choice of encounter data set. The results of this study may inform RTCA SC-228 in terms of validating sensor uncertainty requirements in the Phase 2 MOPS and provide supporting data to the FAA's system safety assessment.

Future research may include evaluation of multi-state noise mitigation methods, such as the Virtual Intruder State Aggregation (VISA) method supported in JADEM. Conceptually this method is similar to a special case of alpha-beta filter, known as the alpha-filter [9]. VISA is currently being investigated and has been shown to have potential in exceeding SUM performance.

Acknowledgments

References

[1] *Integration of Civil Unmanned Aircraft Systems (UAS) in the National Airspace System (NAS) Roadmap*, 2nd ed., Federal Aviation Administration, Washington, DC, 2018.

[2] SC-228, *Minimum Operational Performance Standards (MOPS) for Detect and Avoid (DAA) Systems (DO-365)*, RTCA, Washington, DC, 2017.

[3] SC-228, *Minimum Operational Performance Standards (MOPS) for Air-to-Air Radar for Traffic Surveillance (DO-366)*, RTCA, Washington, DC, 2017.

[4] Rohal, P., and Ochodnicky, J., "Radar target tracking by Kalman and particle filter," *Proceedings of 2017 Communication and Information Technologies (KIT)*, IEEE, Vysoke Tatry, Slovakia, 2017.

[5] Zhou, F., Zhou, D., and Yu, G., "Target Tracking in Interference Environments Reinforcement Learning and Design for Cognitive Radar Soft Processing," *Proceedings of 2008 Congress on Image and Signal Processing*, IEEE, Sanya, Hainan, China, 2008.

[6] Arulampalam, M., Maskell, S., Gordon, N., and Clapp, T., "A tutorial on particle filters for online nonlinear/non-Gaussian Bayesian tracking," *Proceedings of IEEE Transactions on Signal Processing*, Vol. 50, IEEE, 2002, pp. 174–188.

[7] Hue, C., Cadre, J.-P. L., and Perez, P., "Sequential Monte Carlo methods for multiple target tracking and data fusion," *Proceedings of IEEE Transactions on Signal Processing*, Vol. 50, IEEE, 2002, pp. 309–325.

[8] Yang, C., Mohammadi, A., and Chen, Q., "Multi-Sensor Fusion with Interaction Multiple Model and Chi-Square Test Tolerant Filter," *Sensors (Basel)*, Vol. 16, PMC, 2016.

[9] Kalata, P. R., "The Tracking Index: A Generalized Parameter for $\alpha - \beta$ and $\alpha - \beta - \gamma$ Target Trackers," *Proceedings of IEEE Transactions on Aerospace and Electronic Systems*, Vol. AES-20, IEEE, 1984, pp. 174–182.

[10] Zarchan, P., and Musoff, H., *Fundamentals of Kalman Filtering: A Practical Approach*, Vol. 190, AIAA, 2000.

[11] Zulkifley, M. A., and Moran, B., "Robust hierarchical multiple hypothesis tracker for multiple-object tracking," *Expert Systems with Applications*, Vol. 39, 2012, pp. 12319–12331.

[12] Olson, W., "ACAS Xu UAS Detect and Avoid Solution," *Proceedings of Lincoln Laboratory Air Traffic Control Workshop 2016 - 2*, 2016.

[13] Chryssanthacopoulos, J. P., and Kochenderfer, M. J., "Accounting for State Uncertainty in Collision Avoidance," *Journal of Guidance, Control and Dynamics*, Vol. 34, AIAA, 2011, pp. 951–960.

[14] Johnson, M., Mueller, E. R., and Santiago, C., "Characteristics of a Well Clear Definition and Alerting Criteria for Encounters between UAS and Manned Aircraft in Class E Airspace," *Proceedings of the Eleventh USA/Europe Air Traffic Management Research and Development Seminar (ATM2015)*, Lisbon, Portugal, 2015.

[15] *Code of Federal Regulation, General Operating and Flight Rules, title 14, sec. 91.113*, United States Department of Transportation: United States Federal Aviation Administration, ????

[16] Wu, M. G., Lee, S., and Cone, A. C., "Detect and Avoid Alerting Performance with Limited Surveillance Volume for Non-Cooperative Aircraft," *AIAA Scitech 2019 Forum*, 2019. URL `https://arc.aiaa.org/doi/pdf/10.2514/6.2019-2073`.

[17] Theunissen, E., Suarez, B., and Kirk, K., "Development, Integration and Testing of a Stand-Alone CDTI with Conflict Probing Support," *Proceedings of the AIAA Infotech Aerospace Conference*, AIAA, Garden Grove, California, 2012.

[18] Abramson, M., Refai, M., and Santiago, C., "The Generic Resolution Advisor and Conflict Evaluator (GRACE) for Unmanned Aircraft Detect-And-Avoid Systems," Tech. Rep. NASA/TM-2017-219507, NASA Ames Research Center, Moffett Field, California, 2017.

[19] Muñoz, C., Narkawicz, A., Hagen, G., Upchurch, J., Dutle, A., and Consiglio, M., "DAIDALUS: Detect and Avoid Alerting Logic for Unmanned Systems," *Proceedings of the 34th Digital Avionics Systems Conference*, IEEE/AIAA, Prague, Czech Republic, 2015.

[20] *Introduction to TCAS II Version 7.1*, United States Department of Transportation: United States Federal Aviation Administration, Washington, DC, 2011.

[21] Davies, J. T., and Wu, M. G., "Comparative Analysis of ACAS-Xu and DAIDALUS Detect-and-Avoid Systems," Tech. Rep. NASA/TM–2018–219773, NASA Ames Research Center, Moffett Field, California, 2018.

[22] Narkawicz, A., Muñoz, C., and Dutle, A., "Sensor Uncertainty Mitigation and Dynamic Well Clear Volumes in DAIDALUS," *Proceedings of the 37th Digital Avionics Systems Conference*, IEEE, London, UK, 2018.

[23] Jack, D. P., Hoffler, K. D., and Sturdy, J. L., "Mitigating the Impact of Sensor Uncertainty on Unmanned Aircraft Operations," Tech. Rep. NASA CR 2017, NASA Langley Research Center, Hampton, VA, 2017.

[24] Ghatas, R. W., Jack, D. P., Tsakpinis, D., Vincent, M. J., Sturdy, J. L., Munoz, C. A., Hoffler, K. D., Dutle, A. M., Myer, R. R., DeHaven, A. M., Lewis, E. T., and Arthur, K. E., "Unmanned Aircraft Systems Minimum Operational Performance Standards End-to-End Verification and Validation (E2-V2) Simulation," Tech. Rep. NASA/TM-2017-219598, NASA Langley Research Center, Hampton, VA, 2017.

[25] Ghatas, R. W., Tsakpinis, D., Sturdy, J. L., Jack, D. P., Myer, R. R., and DeHaven, A. M., "The Effects of Severity of Losses of Well Clear on Minimum Operations Performance Standards End-to-End Verification and Validation Simulation Study for Integrating Unmanned Aircraft Systems into the National Airspace System using Detect and Avoid Systems," *Proceedings of the 2018 AIAA Information Systems-AIAA Infotech @ Aerospace*, AIAA, Kissimmee, FL, 2018.

[26] Ayyalasomayajula, S., Wieland, F., Trani, A., and Hinze, N., "Unmanned Aircraft System Demand Generation and Airspace Performance Impact Prediction," *Proceedings of the 32nd IEEE Digital Avionics Systems Conference*, IEEE, Syracuse, NY, 2013.

[27] Park, C., Lee, H., and Musaffar, B., "Radar Data Tracking Using Minimum Spanning Tree-Based Clustering Algorithm," *Proceedings of 11th AIAA Aviation Technology, Integration, and Operations (ATIO) Conference*, AIAA, Virginia Beach, VA, 2011.

[28] Kochenderfer, M. J., Kuchar, J. K., Espindle, L. P., and Griffith, J., "Uncorrelated Encounter Model of the National Airspace System, Version 1.0," Tech. Rep. ATC-345, MIT Lincoln Laboratory, Lexington, Massachusetts, 2008.

[29] Wu, M., and Lee, S., "Impact of Sensor Uncertainties on Detect-and-Avoid Systems' Separation Performance," *2020 AIAA Aviation Forum*, AIAA, Reno, NV (In Press), 2020.

[30] Bageshwar, V. L., and Euteneuer, E. A., "Multi-Intruder Aircraft, Multi-Sensor Tracking System," *Proceedings of the 34th Digital AvionicsSystems Conference (DASC)*, IEEE/AIAA, Prague, Czech Republic, 2015, pp. 5A5–1–13.

[31] Weinert, A. J., Harkleroad, E. P., Grith, J., Edwards, M. W., and Kochenderfer, M. J., "Uncorrelated Encounter Model of the National Airspace System, Version 2.0," Tech. Rep. ATC-404, MIT Lincoln Laboratory, Lexington, Massachusetts, 2013.